Thermionic tunneling through Coulomb barriers in charged self-assembled quantum dots

A. Schramm
Optoelectronics Research Centre, Tampere University of Technology, FIN-33101 Tampere, Finland and Institute of Applied Physics, University of Hamburg, D-20355 Hamburg, Germany

S. Schulz, T. Zander, Ch. Heyn, and W. Hansen
Institute of Applied Physics, University of Hamburg, D-20355 Hamburg, Germany

(Received 7 April 2009; revised manuscript received 21 July 2009; published 12 October 2009)

The temperature and electric-field dependence of the electron emission from charged semiconductor quantum dots is studied with transient capacitance spectroscopy. The self-assembled InAs quantum dots are embedded within Schottky diodes grown with molecular-beam epitaxy on GaAs(001). In accordance with the different activation energies the emission from the *s* and the *p* shell of the quantum dots takes place with strongly different rates. In addition, the emission rates depend on the charge state of the shells. The behavior can quantitatively be understood with a thermionic-tunneling model in which the tunnel barrier is assumed to consist of a Coulomb barrier arising from the charge within the dot and a triangular contribution from remote charges.

DOI: 10.1103/PhysRevB.80.155316 PACS number(s): 73.21.La, 73.63.Kv, 73.90.+f

I. INTRODUCTION

The complex interplay of quantization and interaction in semiconductor nanostructures is found to result in a wealth of intriguing properties that can be employed in applications such as single-photon emitters, detectors or even quantum computing and cryptographic devices. In self-assembled InAs quantum dots (QDs) both effects are of the same order. As determined, e.g., by capacitance-voltage spectroscopy[1–4] typical values for the *s*-*p* level separation and the Coulomb-blockade energy of electron states in InAs QDs are 40–60 meV and 20 meV, respectively. These values are essential for the understanding of, e.g., Raman and photoluminescence experiments[5,6] and for the development of applications in optoelectronic devices such as quantum-dot photodiodes for coherent optoelectronics,[7,8] photodetectors,[9,10] and basic memory devices.[11,12] In the latter cases the QDs are embedded in diode-like devices and the QDs are exposed to strong electric fields. Furthermore, devices utilizing QDs are generally supposed to work at temperatures at which thermal effects are important. Appenzeller *et al.*[13] have pointed out the importance of thermionic emission for devices employing one-dimensional semiconductors. Despite its importance for applications the field-dependent emission and capture of charge carriers in quantum dots is only barely studied so far.[14–18]

It has been pointed out that the emission and capture of charge carriers can be quite complex since several emission (capture) paths can be involved.[19] Generally, for the escape of electrons from QDs embedded in a Schottky diode thermal, tunneling, and thermally assisted tunneling processes may be distinguished[15,17,20–22] as sketched in Fig. 1. Indeed, previous experiments already revealed competition of thermally activated and pure tunneling emission.[23] In thermally assisted tunneling processes the electron tunnels from an intermediate state, which is energetically elevated with respect to the ground state. Activated tunneling from the excited state is favorable with respect to the pure tunneling process because of the strong dependency of the tunnel rate on the barrier height and width. Furthermore, it has been pointed out that not only the resonant quantum-dot states[17,24] can act as intermediate states but also the continuum of evanescent states[15,20,23,25] that arises in an electric field from the conduction band penetrating the barrier. In close analogy to the thermionic tunneling process at Schottky barriers[26] this will lead to a lowering of the apparent activation energy of the emission process, which is strongly dependent on the electric field.[15,27]

The gate-voltage dependence of the apparent activation energy describing the electron emission from quantum dots has previously been studied in transient capacitance spectroscopy experiments.[15,27] With the gate voltage the electric field at the QDs is tuned. The electric field in the vicinity of the QDs can be divided into two contributions. The first one originates from remote charges such as ionized donors of the depletion zone and charges on electrodes. In slightly doped Schottky diodes and in close vicinity to the QD layer the corresponding potential can be described by a triangular contribution to the QD barrier potential with slope set by the reverse voltage, i.e., the voltage applied while the transient is recorded. The second contribution to the electric field is the repulsive Coulomb field induced by the charges occupying the dots. This contribution is controlled by the pulse voltage,

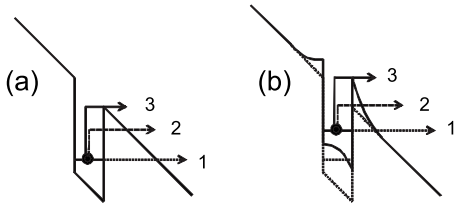

FIG. 1. (a) Conduction-band diagram across a QD in an external electric field in a Schottky diode. Arrows indicate electron emission processes: thermal emission (3, full line), tunneling emission (1, dotted), and thermally assisted tunneling (2, dashed). (b) shows schematically the modification, if the Coulomb potential of charge in the QD contributes to the potential.

i.e., the voltage applied before the transient. During the transient it decreases with the dot occupation. In our previous experiments we found that the field dependence of pure tunneling[22] as well as thermally assisted tunneling[15,27] from the singly occupied *s* shell of the QDs can indeed be well described by a triangular potential in a thermally assisted tunneling (TAT) model. However, if the dot is occupied with several electrons, their repulsive Coulomb field modifies the barrier potential as depicted in Fig. 1(b). In essence, the effective barrier potential for thermally assisted tunneling processes is significantly reduced leading to enhanced rates with increasing shell filling of the QD. In recent publications we studied pure tunneling processes from QDs (Refs. 22 and 23) with a corresponding potential model. In particular, we find that the behavior of the thermal emission from the *p* shell in the presence of a magnetic field can be understood on this footing. Low-temperature pure tunneling data have been analyzed with a Wentzel-Kramers-Brillouin (WKB) approach on the basis of a one-dimensional potential consisting of a triangular and a Coulomb-repulsion contribution. From the thermally assisted emission rates apparent activation energies have been determined with the conventional Arrhenius analysis. From comparison of the data and, in particular, from the magnetic field dependence it is concluded that for emission from *p* states thermally assisted tunneling plays a much more important role compared to *s*-type states. The resolution of the data, however, so far did not suffice to quantitatively analyze the thermal *p*-type emission as function of the external electric field. Improved quality of the samples used in this paper allows us now to perform such a study.

In our paper, we study the electric-field enhanced thermally activated electron emission from charged QDs by means of temperature-dependent transient capacitance experiments, i.e., deep level transient spectroscopy (DLTS). We observe strongly different emission rates for *s*- and *p*-state electrons in good correspondence with level separations determined by different methods, e.g., by capacitance-voltage spectroscopy. Structures in the DLTS spectra reflect the charge state of the QD shell and are explained by the Coulomb-field contribution to the potential landscape in close proximity to the QDs. So far, thermal emission from the *s* shell was analyzed with a TAT model based on a triangular potential barrier, which—as mentioned above—is strictly valid only for the singly occupied *s* shell.[15] Here we analyze the thermal emission from the *s* and *p* shells with a TAT model that considers the repulsive Coulomb contribution to the barrier potential. We call it Coulomb-TAT model. It enables us to quantitatively understand the strong field dependence of the thermal *p*-state emission rates.

II. EXPERIMENTS

The samples were grown by molecular-beam epitaxy on undoped GaAs(001) substrates. In the following we concentrate on the data of a representative device in which the QD layer is embedded in a slightly *n*-doped ($N_D=3.5\times10^{15}$ cm^{-3}) Schottky diode. First, a highly Si-doped GaAs layer ($N_D=3\times10^{18}$ cm^{-3}) was grown, providing a well-conducting back contact, followed by a 1200 nm GaAs:Si ($N_D=3.5\times10^{15}$ cm^{-3}) layer. The QD layer was embedded between 5 and 10 nm undoped GaAs layers in order to prevent a direct doping of the QDs. The QDs were grown at $T=495$ °C with a growth rate of $F=0.01$ ML/s and a coverage $\theta=2.1$ ML. The QDs were covered by 750 nm GaAs:Si ($N_D=3.5\times10^{15}$ cm^{-3}). Finally, for atomic force microscopy (AFM), a second QD layer was deposited on the sample surface using the same growth parameters as for the embedded QDs. The AFM images showed an ensemble of randomly distributed QDs with a narrow size distribution and a density of about 4×10^{9} cm^{-2}. Using standard optical lithography and liftoff techniques, Schottky contacts were formed on top of the sample by evaporation of 50 nm chromium with a diameter of 1 mm. The ohmic back contact was provided by indium alloyed into the highly doped GaAs back contact layer. The DLTS measurements were performed using a Boonton capacitance meter and a helium flow cryostat with variable temperatures between 10 K and room temperature.

III. EXPERIMENTAL RESULTS

The capacitance transients discussed in the following are measured as follows. During a 1 ms long filling voltage pulse V_p applied between the back contact and the metal contact of the diode the dots are charged with electrons. The capacitance transient of the diode is measured after the voltage has been reduced from the pulse voltage to the reverse voltage V_r. At V_r the dot layer is located within the depletion zone, the depth of which depends on the quantum-dot occupation. The measured capacitance transients thus reflect the time evolution of the dot occupation.

In Fig. 2(a) DLTS spectra of the diode recorded at three reverse voltages V_r are presented. The value of V_r determines the strength of the electric field at the quantum-dot layer. The DLTS spectra in Fig. 2 are determined from the capacitance transients using the Double-Boxcar technique[15,28] with a reference time $\tau_{ref}=19$ ms. At $V_r=-1.2$ V we observe two pronounced DLTS maxima at $T\approx70$ K and $T\approx35$ K that we associate with electron emission from the QD *s* and *p* shells, respectively. The splitting of the *s*-shell maximum is attributed to different emission rates of QDs occupied by one and two electrons, respectively.[15,29] Accordingly, a fine structure is resolved in the *p* maximum associated with the emission from quantum dots occupied by one to four electrons in the *p* shell.[29] Whereas we could only resolve one *p* electron in our previous studies on the electric-field dependencies of QD electrons,[15] here the observation of four electrons in the *p* shell will enable us to study the electric-field dependence of the fully loaded *p* shell. At temperatures below $T<20$ K a temperature-independent DLTS signal occurs which is associated with pure tunneling processes.[16,22–24,30] Decreasing V_r (increasing the electric field F) leads to a shift of the *s*-state maximum to lower temperatures as observed in Fig. 2(a). Further on, with increasing electric field the *p* maximum shrinks to a temperature-independent DLTS signal arising from pure tunneling processes.[22] The temperature range in

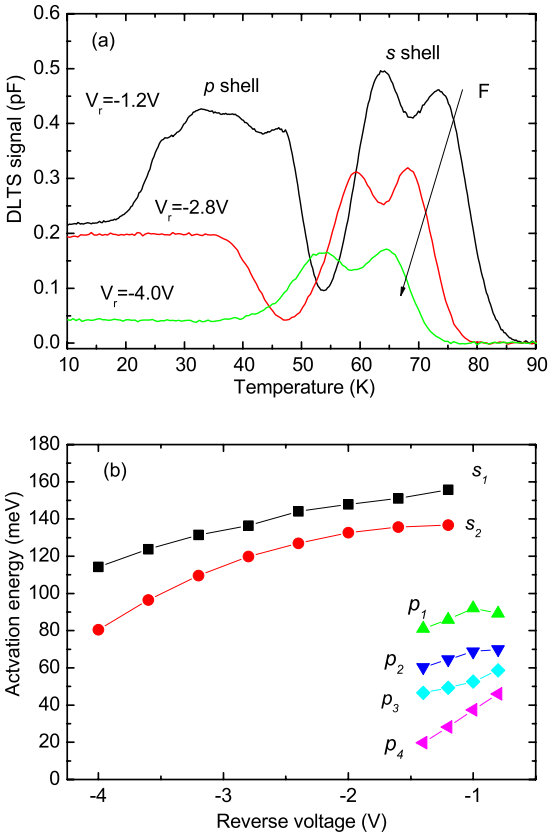

FIG. 2. (Color online) (a) DLTS spectra of a Schottky diode with embedded QDs for various reverse voltages V_r as indicated in the figure. The pulse bias and duration are V_p=0.4 V and t_p =1 ms, respectively. The rate window of the Double-Boxcar filter is τ_{ref}=19 ms with t_2/t_1=8. (b) Activation energies E_a at different V_r.

which the tunneling signals dominate increases with higher electric fields. This behavior points to competition between thermal and tunneling paths in electric fields. Furthermore, we note that the height of the tunneling signals is strongly dependent on the electric field.[22,23]

In a first approach, we determine apparent activation energies E_a with a classical Arrhenius analysis of the DLTS data, i.e., assuming pure thermal excitation. In Fig. 2(b) corresponding apparent activation energies E_a for the s and p maxima at different V_r are depicted. The values of E_a are obtained from a conventional Arrhenius analysis[28] of the DLTS-maxima positions in the spectra recorded at different reference times τ_{ref}. The activation energies significantly decrease with decreasing V_r (increasing electric field). Furthermore, we observe that the field dispersion of the activation energies increases with the occupation state of the quantum dots. In particular, we are able to evaluate the electric-field dependence of the p-state electrons. They show a significantly stronger dispersion in electric field than the s-state electrons. The reverse-voltage range in which the apparent activation energies E_a could be determined is much smaller for the emission from the p shell since at higher electric fields the tunneling signal starts to dominate the DLTS spectra.

IV. DISCUSSION

Although the zero-dimensional quantum-dot states can be considered similar to electron traps in bulk material, they differ in both the confinement potential as well as the charge occupation. It is well known that an electric field lowers the barrier in traps with Coulomb-confinement potential as first discussed by Poole and Frenkel.[31] A similar effect can be expected in confinement potentials of different shapes. In particular, for the case of a rectangular quantum well with width $2z_0$ the barrier lowering can be easily estimated to be eFz_0. The experiments reveal that the field dispersion of the activation energies is much stronger than would be expected from this effect and points to the importance of tunneling processes.[15] The tunneling rate increases exponentially with the electric field since the effective length of the tunnel barrier decreases. Indeed, in previous work[15,23] it has been shown that the behavior of the DLTS signal associated to the s-shell emission can be explained with a TAT model that had been developed to explain the electric-field-dependent emission rates from deep impurity states in semiconductors.[20,32–34] In the model the emission from the quantum dot due to purely thermal emission as well as competing thermally assisted tunneling was considered in a simple one-dimensional approximation with a triangular tunnel barrier.

In case of purely thermal emission described by an Arrhenius law the activation energy E_a and the capture cross section σ_a are determined from the temperature dependence of the emission rate

$$e_{\mathrm{th}}(T) = \sigma_a \gamma T^2 \exp(-E_a/kT), \tag{1}$$

where γ is a temperature-independent constant and k is the Boltzmann constant. The tunneling emission rate e_{tu} is approximated within a one-dimensional, semiclassical WKB approach[22,23,35]

$$e_{\mathrm{tu}} = e_{\mathrm{tu},0}(F)\exp\left[-\frac{\sqrt{8m^*}}{\hbar}\int_0^{z_1}\sqrt{V_B(z)}dz\right]. \tag{2}$$

The pre-exponential factor $e_{\mathrm{tu},0}$ is assumed to be only moderately field dependent as in the case of a Dirac well, where it is linear.[20] Furthermore, m^* is the effective mass of the barrier material, $\hbar$ is Planck's constant, and $V_B(z)$ is the barrier potential along the (reverse) growth direction. The barrier potential depends on the electric field F and the energy of the tunneling electron, which is assumed to remain constant during the tunneling process. The integration spans the nonclassical region between the quantum dot and the point z_1, where the barrier-band edge meets the energy of the tunneling electron. The total emission rate is obtained by summing up all contributions for electron energies E between the top of the quantum-dot potential, i.e., the band-edge energy of the barrier at the location of the quantum dot, and the energy of the s or p state at which the thermally activated tunneling process starts. In the TAT model the enhancement $e_{\mathrm{meas}}/e_{\mathrm{th}}$ with respect to the purely thermal emission can be written as[34]

$$\frac{e_{\text{meas}}}{e_{\text{th}}} = 1 + \int_0^{E_B} \Gamma(E)dE, \tag{3}$$

where E_B is the barrier height with respect to the energy of the state from which the electron escapes and with

$$\Gamma(E) = \frac{1}{kT}\exp\left[\frac{E}{kT} - \frac{\sqrt{8m^*}}{\hbar}\int_0^{z_1}\sqrt{V_B(z)}dz\right]. \tag{4}$$

In Refs. 15 and 27 we used a triangular tunneling barrier potential $V_B(z)$ to calculate the tunneling rate from the intermediate state in the thermally assisted tunneling process (linear TAT model). The slope of the potential was assumed to take into account both the electric field of the space charge in the Schottky diode as well as the field of charges within the dots. In this paper we use a more realistic potential form (Coulomb-TAT model) consisting of a linear part and a Coulomb potential[22,23]

$$V_B(z) = E - eFz - \frac{ie^2}{4\pi\varepsilon\varepsilon_0}\left[\frac{1}{z_0} - \frac{1}{z_0 + z}\right]. \tag{5}$$

Here, e is the electron charge, ε and ε_0 are the dielectric constants of GaAs and vacuum. The last term is the Coulomb potential of the charge in the quantum dots, which are modeled by metallic spheres with center at $z=-z_0$ and radius z_0. The integer i denotes the dot electron occupation after the emission process. The linear part eFz arises from the space charge in the Schottky diode and can be controlled by the diode bias,

$$F = \frac{eN_D}{\varepsilon\varepsilon_0}\left(\sqrt{\frac{2}{eN_D}[\varepsilon\varepsilon_0(V_{\text{bi}} - V_r) + ien_Q z_Q]} - z_Q\right), \tag{6}$$

where n_Q is the areal quantum-dot density, V_r is the bias, and V_{bi} the built-in voltage of the Schottky diode. We note that the linear TAT model is obtained with $i=0$ in Eq. (5). The Coulomb contribution in Eq. (5) approximates the field of the charge in the QD from which the considered emission takes place. In contrast, the second term in the square root of Eq. (6) takes into account the average field of the charges in all remote QDs. As will be seen in the following, the most important contributions $\Gamma(E)$ to the integral Eq. (3) will be at energies close to the band-edge energy of the barrier. We thus may expect that, for the calculation of the emission rate from a highly charged QD with a TAT model, the Coulomb part in Eq. (5) describing the potential in close proximity to the QD is very important.

To demonstrate the emission-rate enhancement in electric fields, we first show in Fig. 3(a) numerical calculations of the TAT contribution $\Gamma(E)$ to the emission at energy E for singly occupied QDs ($i=0$) at different temperatures and electric fields as indicated in the figure. The parameters N_D, E_B, and the temperatures are chosen close to the experimental data. We observe a strong temperature effect. With decreasing temperature $\Gamma(E)$ strongly increases and the maximum of $\Gamma(E)$ moves toward higher E, i.e., more states at larger distance from the band edge of the barrier contribute to the emission probability. Qualitatively, the behavior is similar to the case of a triangular potential, where $\Gamma(E)$ is proportional

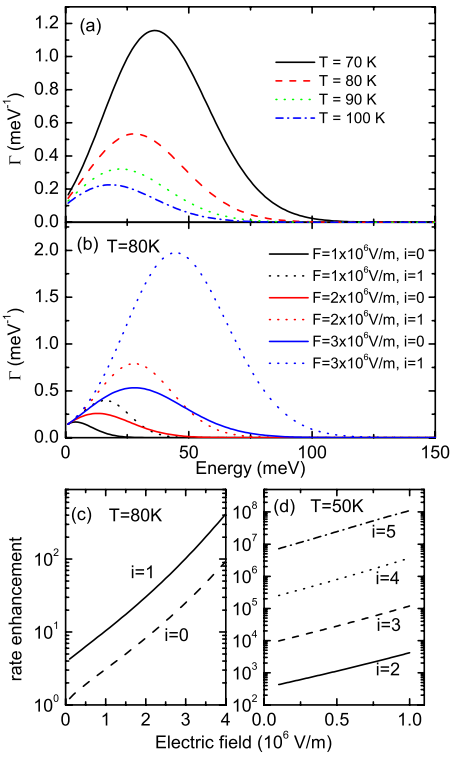

FIG. 3. (Color online) (a) Calculated values of the integrand Γ of Eq. (3) for nonoccupied QDs ($i=0$) at different temperatures as indicated in the figure. Further model parameters, similar to the experiment, are $E_B=150$ meV, $z_0=6$ nm, and $F=3\times10^6$ V/m. (b) shows calculations for Γ for nonoccupied QDs ($i=0$, full line) and singly charged QDs ($i=1$, dotted line) at different field strength. In (c) the theoretical emission-rate enhancement $e_{\text{meas}}/e_{\text{th}}$ versus the electric field at $T=80$ K with same parameters as in (a). In (d) the emission-rate enhancement $e_{\text{meas}}/e_{\text{th}}$ at $T=50$ K, $z_0=6$ nm and $E_B=110$ meV is displayed for p-electron emission from QDs.

to the product of an exponentially decreasing tunnel probability and the exponentially increasing thermal activation probability.[25] In Fig. 3(b) the Coulomb-barrier effect of charged QDs on the emission-rate enhancement is demonstrated for singly ($i=0$) and doubly charged QDs ($i=1$) at different field strengths. The data show that in case of dots occupied with two electrons in the s shell ($i=1$) the emission rates are strongly enhanced as compared to singly occupied QDs. For example, at an electric field of $F=2\times10^6$ V/m we obtain for $i=0$ and $i=1$ emission-rate enhancement factors of 8.3 and 30.2, respectively. Qualitatively, the enhancement is readily explained as a consequence of Coulomb repulsion of the QD charge. This behavior holds for the whole field range depicted in Fig. 3(c). Figure 3(d) demonstrates that the emission-rate enhancement further increases when the QDs are charged with more than two electrons and the emission starts from the p shell.

In Fig. 4 we present activation energies determined from the emission-rate analysis within different models. At each value of the electric field a set of experimental emission rates is measured at different reference times. Filled symbols denote apparent activation energies determined from a conventional Arrhenius analysis of the thus determined temperature dependence of the emission rates. Obviously, the apparent

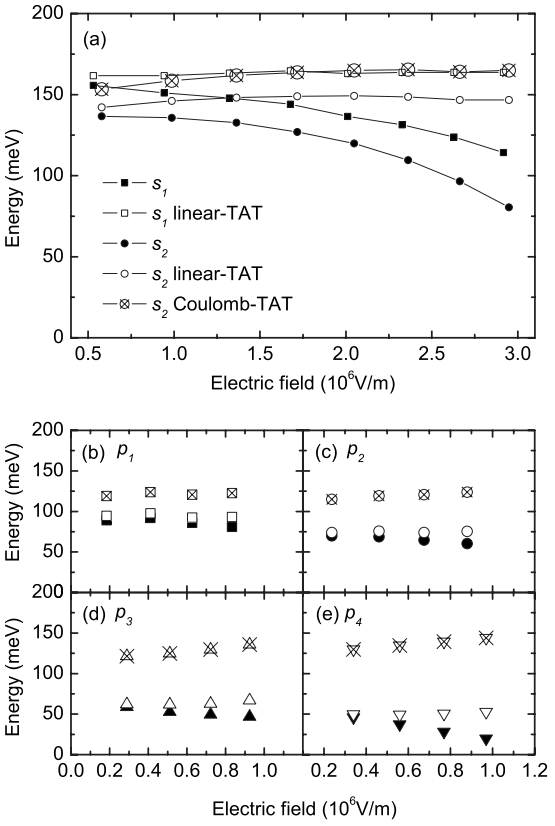

FIG. 4. (a) Apparent activation energies E_a (filled data points) of the s_1 (square) and the s_2 electron (circle) obtained with a conventional Arrhenius analysis from the experimental capacitance transients at different electric-field strengths controlled by V_r. Also depicted are the barrier heights E_B (corresponding open data points) obtained from the linear TAT model (i=0). The crossed data points are the energies of the s_2 electron derived from the Coulomb-TAT model which includes the Coulomb contribution to the tunneling barrier. [(b)–(e)] Activation energies E_a (filled data points), barrier heights E_B (corresponding open data points) obtained from the TAT model, and energies (crossed data points) obtained from the Coulomb-TAT model of p-state electrons as indicated in the figure.

activation energies strongly depend on the occupation state of the QDs as well as the electric field at the QDs. The crossed data points are evaluated with the Coulomb-TAT model from the experimental data as follows. First, from the experimental rates and the apparent activation energy a rate enhancement according to Eq. (3) is calculated solving numerically the integral Eq. (3). The calculated emission rates e_{th} are used for a second Arrhenius analysis in order to determine new activation energies. These energies are used for a next iteration until the energies used in Eq. (3) and determined from the Arrhenius analysis of the calculated emission rates e_{th} are consistent. Finally, the thus determined activation energy should resolve the true barrier height E_B as measured from the quantum-dot state, from which the electron escapes. One and up to four iteration steps are needed to calculate E_B for the s and the p electrons, respectively. The thus determined barrier heights E_B are depicted in Fig. 4(a) for the s_1- and s_2-state electrons. For both occupation states the barrier height is close to 163 meV. Furthermore, the barrier height is almost independent on the electric field at the quantum dot. Both facts indicate that in the applied emission model the electron interaction in multiply occupied dots as well as the effect of an external electric field have been properly taken into account. In particular, the electron interaction is considered via a quantum capacitance estimated from the shape of the dot: if the occupation of the dot changes, all single-particle energy levels shift by the same amount estimated from a spherical metal capacitor with radius z_0. It is assumed that the significant electron interaction effects can be described with this shift. The potential step defining the dot boundary has to be localized to a length scale much smaller than the scale on which the Coulomb potential decreases. In particular, in this approach the energy shift does not alter the relative energy distances between the single-particle levels and the height of the barrier at the dot boundary. E.g., in this model the height of the barrier with respect to the s level does not depend on the occupation of the level. The repelling potential arising from the charge in the QDs lifts the whole conduction band including the free-energy position of the s shell. Correspondingly, assuming a purely thermal emission process, Engström *et al.*[36] have pointed out that the Coulomb-charging energy is not expected to influence the activation energy in DLTS measurements. This point is also obvious from Fig. 1(b). The crossed data points in Fig. 4 refer to the height of the barrier with respect to the s or p levels and thus in our model should not depend on the occupation. In essence, they are calculated with our TAT model from the experimentally determined apparent activation energies by subtraction of the TAT contribution from the data. While due to the tunneling contribution the apparent activation energies depend on the electric field and the dot occupation, the calculated barrier heights do not.

We note that in the linear TAT model the dependence on an external electric field was already well described for the s emission.[15,27] However, in that model the barrier heights still seem to be dependent on the occupation state. Data points obtained from the linear TAT model are indicated by open symbols in Fig. 4(a). Of course, the linear and Coulomb-TAT data are identical for the s_1 emission.

In Figs. 4(b)–4(e) the corresponding apparent activation energies and calculated barrier heights for emission from the p shell are presented. We note that the field dispersion of the apparent activation energies is much stronger than in the case of the emission from the s shell as can be seen from the data in Fig. 2(b). As noted above, the strong field dependence already indicates the importance of tunneling processes. Also, from the discussion of the calculated emission-rate enhancements depicted in Fig. 3(d) we expect that the rate for emission from the p shell is drastically enhanced because of the lower effective barrier and the repulsive Coulomb field of the dot charges. Indeed, the barrier heights E_B determined within the Coulomb-TAT model are considerably higher than the apparent activation energies and the difference increases with the charge state of the p shell. As in the case of the s-shell emission, the barrier heights denoted by crossed symbols in Figs. 4(b)–4(e) are determined with the Coulomb-TAT model. The open symbols calculated with the linear TAT model demonstrate the increasing importance of the Coulomb potential if the QDs are occupied with more elec-

trons. While the electric-field dependence is already well accounted for, the barrier heights still strongly differ in this model. As in the case of the *s*-shell emission, the barrier heights determined with the Coulomb-TAT model for the p_1 electron [Fig. 4(b)] are nearly independent on the electric field. The barrier energies determined for dots with a higher electron number in the *p* shell slightly increase at higher fields as can be observed in Figs. 4(c)–4(e). This remaining slight increase in the barrier energies with the electric field might originate from a field dependence of the effective dot confinement potential and a correspondingly modified z_0. The barrier heights extrapolated to zero electric field average to a value of 121 meV almost independent on the charge state of the *p* shell. Thus, in a simple single-particle model, these data yield an energetic difference of 42 meV between the *s* and *p* shell in good correspondence with values determined on similar quantum dots with different techniques.[1–3]

V. CONCLUSION

To conclude, thermally activated emission processes from charged self-assembled InAs QDs are studied. The QDs are embedded in *n*-doped Schottky diodes. We discuss the influence of the Coulomb barrier on the electron emission of multiply charged QDs. From experimental capacitance transients we obtain apparent activation energies that strongly depend on the shell from which the emission takes place, the charge state of the quantum dot and the external electric field controlled by the diode bias voltage. The charge-state and field dependence can be well accounted for by a two-step thermally assisted tunneling model. Here we assume thermal excitation to an intermediate state from which the electron tunnels through the remaining barrier. For the calculation of the tunneling probability a one-dimensional WKB approach has been employed. The results clearly demonstrate that it is essential to consider the Coulomb contributions of the charges in the QD to the barrier potential.

ACKNOWLEDGMENT

The authors acknowledge the Deutsche Forschungsgemeinschaft (DFG) for financial support via SFB 508 "Quantum materials."

[1] H. Drexler, D. Leonard, W. Hansen, J. P. Kotthaus, and P. M. Petroff, Phys. Rev. Lett. **73**, 2252 (1994).
[2] B. T. Miller, W. Hansen, S. Manus, R. J. Luyken, A. Lorke, J. P. Kotthaus, S. Huant, G. Medeiros-Ribeiro, and P. M. Petroff, Phys. Rev. B **56**, 6764 (1997).
[3] R. J. Warburton, B. T. Miller, C. S. Dürr, C. Bödefeld, K. Karrai, J. P. Kotthaus, G. Medeiros-Ribeiro, P. M. Petroff, and S. Huant, Phys. Rev. B **58**, 16221 (1998).
[4] D. Reuter, P. Kailuweit, A. D. Wieck, U. Zeitler, O. Wibbelhof, C. Meier, A. Lorke, and J. C. Maan, Phys. Rev. Lett. **94**, 026808 (2005).
[5] M. Ediger, G. Bester, A. Badolato, P. M. Petroff, K. Karrai, A. Zunger, and R. J. Warburton, Nat. Phys. **3**, 774 (2007).
[6] P. A. Dalgarno, J. M. Smith, J. McFarlane, B. D. Gerardot, K. Karrai, A. Badolato, P. M. Petroff, and R. J. Warburton, Phys. Rev. B **77**, 245311 (2008).
[7] A. Zrenner, E. Beham, S. Stufler, F. Findeis, M. Bichler, and G. Abstreiter, Nature (London) **418**, 612 (2002).
[8] M. M. Vogel, S. M. Ulrich, R. Hafenbrak, P. Michler, L. Wang, A. Rastelli, and O. G. Schmidt, Appl. Phys. Lett. **91**, 051904 (2007).
[9] M. Grundmann, *Nano-Optoelectronics* (Springer, New York, 2002).
[10] D. J. Mowbray and M. S. Skolnick, J. Phys. D **38**, 2059 (2005).
[11] C. Balocco, A. M. Song, and M. Missous, Appl. Phys. Lett. **85**, 5911 (2004).
[12] M. Geller, A. Marent, T. Nowozin, D. Bimberg, N. Akcay, and N. Öncan, Appl. Phys. Lett. **92**, 092108 (2008).
[13] J. Appenzeller, M. Radosavljevic, J. Knoch, and P. Avouris, Phys. Rev. Lett. **92**, 048301 (2004).
[14] W.-H. Chang, W. Y. Chen, T. M. Hsu, N.-T. Yeh, and J.-I. Chyi, Phys. Rev. B **66**, 195337 (2002).
[15] S. Schulz, S. Schnüll, C. Heyn, and W. Hansen, Phys. Rev. B **69**, 195317 (2004).
[16] M. Geller, E. Stock, C. Kapteyn, R. L. Sellin, and D. Bimberg, Phys. Rev. B **73**, 205331 (2006).
[17] O. Engström, M. Kaniewska, W. Jung, and M. Kaczmarczyk, Appl. Phys. Lett. **91**, 033110 (2007).
[18] T. Nowozin, A. Marent, M. Geller, D. Bimberg, N. Akcay, and N. Öncan, Appl. Phys. Lett. **94**, 042108 (2009).
[19] O. Engström and P. T. Landsberg, Phys. Rev. B **72**, 075360 (2005).
[20] G. Vincent, A. Chantre, and D. Bois, J. Appl. Phys. **50**, 5484 (1979).
[21] M. Gonschorek, H. Schmidt, J. Bauer, G. Benndorf, G. Wagner, G. E. Cirlin, and M. Grundmann, Phys. Rev. B **74**, 115312 (2006).
[22] S. Schulz, A. Schramm, C. Heyn, and W. Hansen, Phys. Rev. B **74**, 033311 (2006).
[23] A. Schramm, S. Schulz, C. Heyn, and W. Hansen, Phys. Rev. B **77**, 153308 (2008).
[24] C. M. A. Kapteyn, F. Heinrichsdorff, O. Stier, R. Heitz, M. Grundmann, N. D. Zakharov, D. Bimberg, and P. Werner, Phys. Rev. B **60**, 14265 (1999).
[25] S. K. Zhang, H. J. Zhu, F. Lu, Z. M. Jiang, and X. Wang, Phys. Rev. Lett. **80**, 3340 (1998).
[26] S. M. Sze, *Semiconductor Devices, Physics and Technology* (John Wiley & Sons, New York, 1985).
[27] S. Schulz, A. Schramm, T. Zander, C. Heyn, and W. Hansen, AIP Conf. Proc. **772**, 807 (2005).
[28] D. V. Lang, J. Appl. Phys. **45**, 3023 (1974).
[29] A. Schramm, S. Schulz, J. Schaefer, T. Zander, C. Heyn, and W. Hansen, Appl. Phys. Lett. **88**, 213107 (2006).
[30] O. Engström, M. Kaniewska, M. Kaczmarczyk, and W. Jung, Appl. Phys. Lett. **91**, 133117 (2007).
[31] J. Frenkel, Phys. Rev. **54**, 647 (1938).

[32] S. Makram-Ebeid and M. Lannoo, Phys. Rev. Lett. **48**, 1281 (1982).
[33] S. Makram-Ebeid and M. Lannoo, Phys. Rev. B **25**, 6406 (1982).
[34] P. A. Martin, B. G. Streetman, and K. Hess, J. Appl. Phys. **52**, 7409 (1981).
[35] A. Patane, R. J. Hill, L. Eaves, P. C. Main, M. Henini, M. L. Zambrano, A. Levin, N. Mori, C. Hamaguchi, Y. V. Dubrovskii, E. E. Vdovin, D. G. Austing, S. Tarucha, and G. Hill, Phys. Rev. B **65**, 165308 (2002).
[36] O. Engström, M. Malmkvist, Y. Fu, H. O. Olafson, and E. O. Sveinbjörnsson, Appl. Phys. Lett. **83**, 3578 (2003).